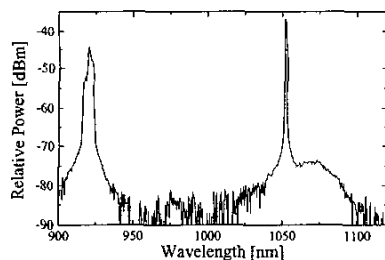


ThGG26 Fig. 1. Schematic structure of the proposed fiber laser cavity.

and silica clad. The Yb-doped double clad fiber was also adiabatically tapered into 125 μm diameter and spliced with the Bragg-grating-imprinted fiber. The tapered region was maintained into the bare-fiber state to guide pump power without the leakage of cladding mode. After the Bragg grating zone, the pump is absorbed in the Yb-doped core along the fiber of 4 m long providing population inversion in Yb ions. The two tapered fibers and grating section was protected with a silica tube to hold air gap and to prohibit contaminations. The end of DCF was cleaved at 90 degree (providing 4% Fresnel reflection serving as an output-coupler of the laser cavity). The pumping source coupled into SMA patch code is operated at the wavelength of 0.92 μm , and its maximum power is about 11 Watt. Experimentally the total cavity loss including DCF was measured about 2.4 dB at wavelengths where optical power was not absorbed by Yb ions in the core, thus the incoming coupled pump power into DCF was about 6.3 Watt. This packaging loss of pump beam was mainly induced by the loss factors such as dusts on tapered zones and differences between fiber parameters. After the tapered zone, the pump beam was absorbed in the Yb-doped core with the length of 4 m. Note that in the tapered section varying cladding shape the pump power will experience mode scrambling to enhance pump absorption into the core. When pumped, emission from Yb ions propagates through the single mode core along the composite cavity. The laser signal is reflected at the grating section with bandwidth of 0.2 nm, propagates the middle section of DCF, and then emits out from cleaved ends of DCF providing 4% Fresnel reflection.

Fig. 2 shows the output power spectrum of double clad fiber laser obtained from optical



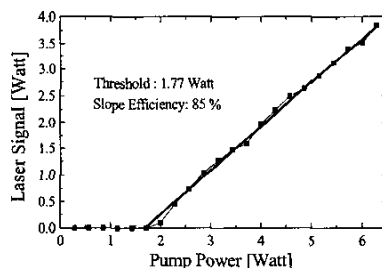
ThGG26 Fig. 2. Laser and pump spectrum measured by optical spectrum analyzer. The absolute power of laser operated at 1.05 μm is 3.8 Watt. The line width is about 0.2 nm.

spectrum analyzer. Due to the OSA power-detecting limit, we added an additional loss to observe the spectrum of the laser; therefore the y-axis value means a relative power not an absolute. When pumped at 6.3 Watt, the coupled pump power had the line width of 10 nm at 0.92 μm , where the absolute power not absorbed by Yb ions was measured about 1.3 Watt. The laser light was shown at the wavelength of 1051 nm with a sharp line width of 0.2 nm. The absolute power reached about 3.8 Watt. The output power characteristic of the proposed fiber laser is shown in Fig. 3. The threshold power to make lasing was about 1.77 Watt. The slope efficiency was about 85%, and the maximum output power was 3.8 Watt for the pump of 6.3 Watt.

In summary, Yb-doped clad-pumped fiber laser with a novel cavity was experimentally demonstrated where two concatenated tapers and the fiber Bragg grating with a sharp bandwidth of 0.2 nm made a high efficient fiber laser. The efficiently packaged cavity showed a low insertion loss of 2.4 dB for fibers with totally different parameters (SMA cable of 700 μm , fiber Bragg grating of 125 μm , and double clad fiber of rectangular structure of 100 by 200 μm^2). The laser output power over 3.8 Watt was obtained with a slope efficiency of 85% and threshold of 1.77 Watt. This laser is applicable to the pumping laser source of thulium-doped fiber amplifier and cascaded Raman lasers. Further optimized cavity parameters to improve laser performances will be presented in detail in the conference.

References

1. H. Po, E. Snitzer, R. Tumminelli, L. Zenteno, F. Hakimi, N.M. Cho, and T. Haw "Double clad high brightness Nd fiber laser pumped



ThGG26 Fig. 3. Laser output for given pumping powers. The maximum output was about 3.8 Watt for the pump of 6.3 Watt, and the slope efficiency was about 85%.

by GaAlAs phased array," in OFC '89 Tech. Dig. 5, 220-223.

2. L. Zenteno, "High-Power Double-Clad Fiber Lasers," *J. Lightwave Technol.* 11(9), 220-223 (1993).
3. H. Jeong, K. Oh, H.S. Seo, S. Choi, and W. Shin, "Enhancement of butt-coupling pump efficiency in a new Nd doped large core double clad fiber laser cavity adiabatically tapered at both ends," in CLEO 2001 Tech. Dig. CWC3.
4. A.S. Kurkov, O.I. Medvedkov, V.I. Karpov, S.A. Vasiliev, O.A. Lexin, and E.M. Dianov, "Photosensitive Yb-doped double-clad fiber for fiber lasers," in OFC '99 Tech. Dig. WM4-1, 205-207.
5. D.J. DiGiovanni, D.P. Jablonowski, and M.F. Yan, "Advances in Fiber Design and Processing," in Chapter 6 of *Optical Fiber Telecommunications IIIA*, I. Kaminow and T.L. Koch, eds. (Academic Press, 1997).

ThGG27

5:30 pm

A stable, dispersion-tuned harmonically mode-locked fiber ring laser using a SOA

Lingze Duan, Christopher J.K. Richardson, Zhaoyang Hu, Mario Dagenais, and Julius Goldhar, *Department of Electrical and Computer Engineering, University of Maryland, College Park, MD 20742, USA, Email: dz@glue.umd.edu*

1. Introduction

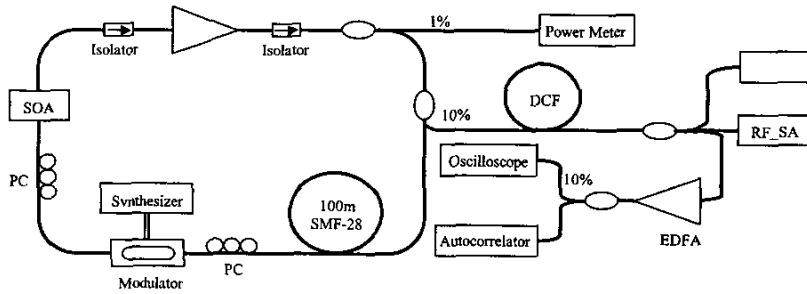
Practical, high-speed optical communication systems require stable, wavelength-tunable, high-speed optical signal generators. Dispersion-tuned harmonically mode-locked fiber ring lasers (HMLFRLs) have been proved to be able to achieve high repetition rate and smooth wavelength tuning.^{1,2} However, harmonic mode locking often causes supermode noise (SMN).³ Several methods have been proposed to suppress the SMN.⁴⁻⁶ But either high optical power or a complex electro-mechanical feedback system is required for these approaches.

It has been shown that a fast intensity-dependent loss is able to suppress the SMN.⁴ It is possible that a fast intensity-dependent gain can also suppress the SMN. Semiconductor optical amplifiers (SOAs) are highly nonlinear devices with fast recovery times (~ 1 ns). Gain Saturation in SOAs provides the intensity-dependent gain, which is used for SMN suppression.⁷

In this paper, we report a dispersion-tuned HMLFRL incorporating a SOA. The combined effects of group velocity dispersion (GVD) and the SOA were studied numerically and experimentally. Comparisons showed that the SMN was significantly reduced by the introduction of the SOA.

2. Experiment and Results

A schematic of the experimental setup is shown in Fig. 1. The ring cavity consisted of an EDFA, a SOA, an electro-optic modulator, 100 meter of SMF-28 fiber and a few isolators and polarization controllers (PCs). The total length of the loop was about 150 m, giving a 1.38 MHz cavity mode. The EDFA provided the majority of the total gain. The SOA was biased in its low-gain regime to prevent excessive nonlinear chirp. The Modulator was driven by a synthesized microwave generator at 10 GHz, which was approximately the 7250th har-



ThGG27 Fig. 1. The experimental setup: RF??SA, RF spectrum analyzer; OSA, optical spectrum analyzer.

monic of the ring cavity. Dispersion compensating fiber (DCF) was used to compress the chirped output pulses. Note that there was no optical filter in the cavity because the GVD of the loop functioned as a self-tuning filter.

Numerical simulation was carried out to study the temporal and spectral properties of the output pulses. The simulation was based on the Kuizenga-Siegman model.⁸ The pulse duration was assumed much shorter than the carrier lifetime in the SOA. Both the gain saturation and the saturation-induced self-phase modulation (SPM) of the SOA were taken into account. The simulation showed that dispersion tuning can be achieved in both normal and anomalous GVD regimes. In both regimes, the output pulses were generally chirped and can be compressed by fibers with reverse GVD. Moreover, under similar conditions, the compressed pulses from an anomalous-GVD loop are shorter than those from a normal-GVD loop. Our experiment qualitatively verified the simulation results. The anomalous regime was studied in the following experiment because it gave shorter pulses and required less amount of fiber for pulse compression.

The experiment was first conducted without the SOA. The pump current of the EDFA was 115 mA and the average optical power inside the cavity was 8.5 mW (at the output of the EDFA). The modulator was biased at its half-wave voltage (10.5 V) and driven with 15 dBm RF power at 10 GHz. Fig. 2(a) shows the sampling scope trace and the RF spectrum of the output. The SMN was evident: the amplitude of the pulses had a large fluctuation and the side cavity modes were 20 dB below the modulation peak. When operated at 1552 nm, the average full width at the half maximum (FWHM) and the spectral width were 9.53 ps and 0.376 nm, respectively. The time-bandwidth product was 0.45, indicating chirped pulses (Sech² pulses assumed).

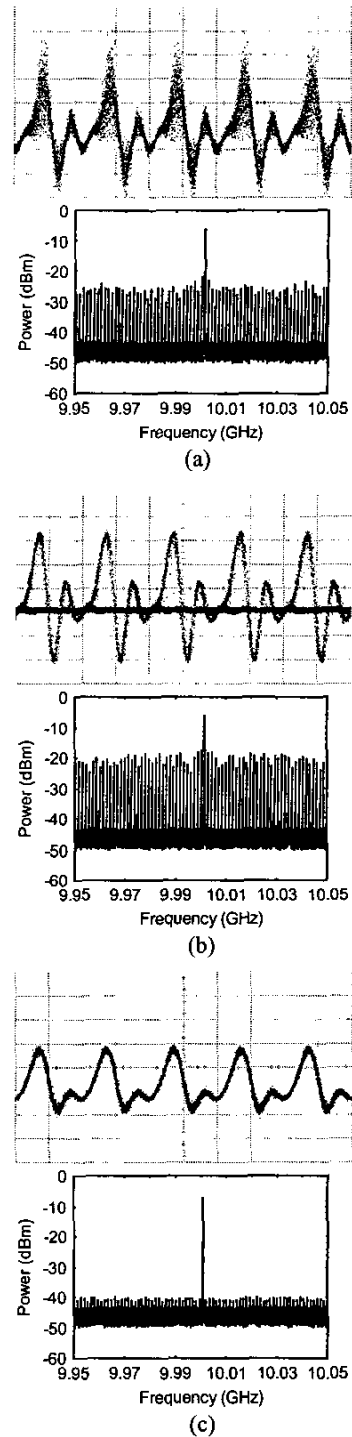
Dispersion tuning was tested by detuning the modulation frequency. When the frequency was increased, the center wavelength blue-shifted linearly, indicating a fixed anomalous GVD, while the spectral width and the sampling scope trace had little change. Fig. 3 shows the relation of the center wavelength versus the frequency detuning. A 0.45-MHz frequency tuning range and a 20-nm wavelength range were achieved.

A unique state was found in the tuning experiment. At 9,999.215 MHz (wavelength 1561.5 nm), the output spectrum became abnormally broad and the sampling scope trace appeared to be a patterned pulse train, with all the pulses having the same amplitude, as shown in Fig. 2(b). A

1.9-ps FWHM and a 1.48-nm spectral width were measured, giving a 0.34 time-bandwidth product, which is very close to 0.31 for transform-limited pulses. This was believed to be a soliton state, where the SPM of the fiber balanced the anomalous GVD at a certain power level. Those pulses with energy close to this power level in the initial state became solitons, while others were fully suppressed, resulting in a random 0-1 pattern circling in the loop. The histogram of the pulse amplitude showed a significant pulse dropout rate and, as shown in Fig. 2(b), side modes were only 10 dB below the modulation peak. The soliton state was only stable within a 5-KHz frequency range.

With the SOA inserted into the cavity, a different behavior was observed. Using a driving current of 60 mA for the SOA, which was significantly higher than the transparent current (~24 mA) but well below the maximum current 250 mA, and a pump current of 92 mA to the EDFA, the average optical power inside the cavity was kept at 8.5 mW. This selection of driving current was made to ensure that the SOA was operating in the gain regime without introducing an excess amount of nonlinear chirp. The RF power to the modulator remained unchanged. The modulation frequency and the PCs were optimized. As shown in Fig. 2(c), the output pulses had stable amplitude and the side cavity modes were significantly suppressed (about 33 dB below the modulation peak). No pulse dropout occurred as evident from the sampling scope. A FWHM of 26.4 ps and a spectral width of 0.27 nm were measured at 1562 nm, giving a time-bandwidth of 0.88. The output pulses were compressed to 5.3 ps by 225 m DCF and the time-bandwidth product became 0.18, indicating that more power distributed on the spectral wings than normal Sech² pulses.

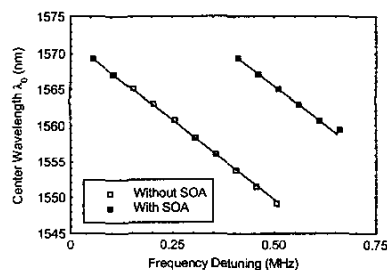
When the modulation frequency was detuned, the center wavelength shifted smoothly and the pulses remained stable. Comparing to the case without the SOA, the tuning curve has the same slope (determined by the intracavity GVD) but a smaller span, as shown in Fig. 3. The smaller tuning range is believed to be a result of the polarization dependence of the SOA. Fig. 4 shows the relation of the rms spectral width versus the center wavelength. The spectral width had little change over the entire tuning range, both with and without the SOA, except in the vicinity of the soliton state. The rms spectral widths of the pulses from the SOA loop were slightly broader than those from the loop without the SOA. This was because of the SPM of the SOA. Note that the rms spectral width was used for comparing the spectra with different shapes. Our measurement also showed



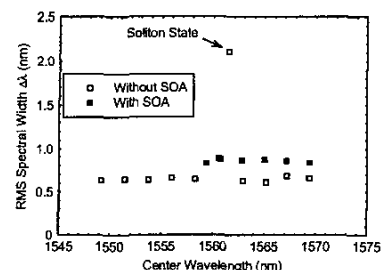
ThGG27 Fig. 2. The sampling scope traces and the RF spectra of the output pulses: (a) without the SOA, (b) in the soliton state and (c) with the SOA.

that the compressed pulse width from the SOA loop remained roughly the same during the wavelength tuning.

It has been observed in our experiment that the SMN can also be suppressed without the SOA, but at a much higher average power, where fiber nonlinearity comes into play.^{1,4,9} Although



ThGG27 Fig. 3. Wavelength tuning: frequency origin is 9,999 MHz without the SOA and 10,000 MHz with the SOA.



ThGG27 Fig. 4. Spectral width vs. center wavelength.

the soliton state mentioned above gave short pulses, it required high power to become dropout-free and was not wavelength tunable. The advantage of using the SOA is to suppress the SMN at a much lower power level while maintaining wavelength tunability.

3. Conclusion

A stable, dispersion-tuned HMLFRL has been demonstrated. SMN was significantly reduced by introducing a SOA into the ring cavity (13-dB improvement in side-mode suppression). Only a 0.25-MHz variation in the modulation frequency was needed to achieve a 10-nm smooth wavelength tuning. Both temporal and spectral widths remained approximately the same during tuning. A 5.3-ps pulse width was obtained at 10 GHz with pulse compression.

References

1. K. Tamura and M. Nakazawa, "Dispersion-tuned harmonically mode-locked fiber ring laser for self-synchronization to an external clock," *Opt. Lett.*, vol. 21, pp. 1984–1986, 1996.
2. C. Shu and Y. Zhao, "Characteristics of dispersion-tuning in harmonically mode-locked fiber laser," *IEEE Photon. Technol. Lett.*, vol. 10, pp. 1106–1108, 1998.
3. G.T. Harvey and L.F. Mollenauer, "Harmonically mode-locked fiber ring laser with an internal Fabry-Perot stabilizer for soliton transmission," *Opt. Lett.*, vol. 18, pp. 107–109, 1993.
4. M. Nakazawa, K. Tamura, and E. Yoshida, "Supermode noise suppression in a harmonically modelocked fibre laser by selfphase modulation and spectral filtering," *Electron. Lett.*, vol. 32, pp. 461–463, 1995.
5. X. Shan and D.M. Spirit, "Novel method to suppress noise in harmonically modelocked

erbium fiber lasers," *Electron. Lett.*, vol. 29, pp. 979–981, 1993.

6. J.S. Wey, J. Goldhar, and G.L. Burdge, "Active harmonic modelocking of an erbium fiber laser with intracavity Fabry-Perot filters," *J. Lightwave Technol.*, vol. 15, pp. 1171–1180, 1997.
7. C. Wu and N.K. Dutta, "High-repetition-rate optical pulse generation using a rational harmonic mode-locked fiber laser," *IEEE J. Quantum Electron.*, vol. 36, pp. 145–150, 2000.
8. D.J. Kuizenga and A.E. Siegman, "FM and AM mode locking of the homogeneous laser—part I: theory," *IEEE J. Quantum Electron.*, vol. QE-6, pp. 694–708, 1970.
9. M. Horowitz, C.R. Menyuk, T.F. Carruthers, and I.N. Duling III, "Pulse dropout in harmonically mode-locked fiber lasers," *IEEE Photon. Technol. Lett.*, vol. 12, pp. 266–268, 2000.

ThGG28

5:30 pm

Single Output Polarization Control of Fiber DFB Laser using Injection Locking

W.H. Chung and H.Y. Tam, *Photonics Research Center, Department of Electrical Engineering, The Hong Kong Polytechnic University, Hong Kong, China, Email: eewhchun@inet.polyu.edu.hk*

L.Y. Chan and P.K.A. Wai, *Photonics Research Center, Department of Electronic and Information Engineering, The Hong Kong Polytechnic University, Hong Kong, China, Email: emwai@polyu.edu.hk*

1. Introduction

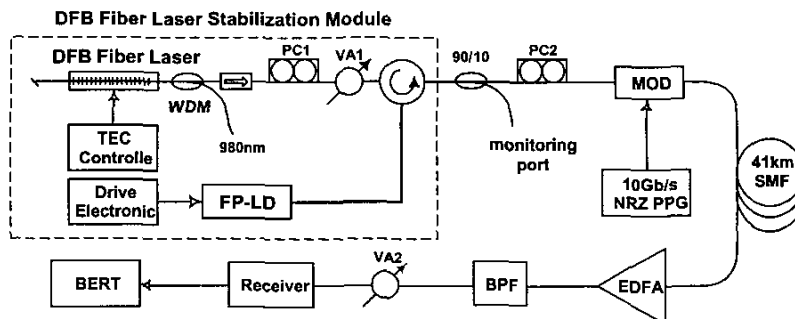
Distributed feedback fiber lasers (DFB-FL) based on fiber Bragg gratings (FBGs) written in Er^{3+} or $\text{Er}^{3+}/\text{Yb}^{3+}$ -doped fibers are promising candidates for optical communication and sensor applications because of their single longitudinal mode output, narrow linewidth, and ease of fabrication with highly accurate lasing wavelength obtained by current phase mask writing method. Most fiber lasers output consists of two orthogonal linear polarizations if they were fabricated with low birefringent fibers. In contrast, single polarization operation is desirable for optical communication applications. Several techniques have been developed to make fiber lasers operate in single polarization. They included twisting the fiber lasers,¹ introducing a birefringence phase-shift in the fiber lasers,² and self-injection locking^{3,4} that

employs a polarization dependent/independent feedback to the cavity. In this paper, we investigated the use of active injection locking technique. By injecting the output of a DFB-FL to a Fabry-Perot laser diode (FP-LD), we showed that stable and highly polarized output can be achieved. A power penalty improvement of 3.8 dB was also demonstrated in a 41-km 10 Gb/s transmission test.

2. Experiments and results

Figure 1 shows the experiment configuration used to stabilize the polarization of a DFB-FL output. The DFB-FL was fabricated by scanning a phase mask in a 5 cm long hydrogenated Er/Yb fiber using a 248 nm excimer laser. We introduced an additional π phase shift in the fiber at 28 mm from the output end by shifting the phase mask half a grating pitch using a high precision piezoelectric stage during the UV scanning process. The lasing wavelength and linewidth of the DFB-FL were 1551.5 nm and less than 500 kHz respectively. The measured linewidth was limited by the spectral linewidth of the tunable diode laser used for heterodyne beating.

Figure 2a shows the output spectrum of the DFB-FL. The output power and side mode suppression ratio (SMSR) of the DFB-FL were 5 mW and 75 dB, respectively. The pump power of the 980 nm pump laser was 70 mW. Dual polarization operation was confirmed by heterodyne beating with a single mode external cavity tunable diode laser using a fast detector. We observed a frequency difference of 850 MHz between the two polarization modes. We then injected the DFB-FL output into the FP-LD using a polarization independent circulator. We monitored the injection locked signal from the output port of the circulator. The FP-LD was a double channel planar buried heterostructure (DC-PBH) type diode laser with a center wavelength of 1548.7 nm and a threshold current (I_{th}) of 11 mA. Figure 2b shows the spectrum of the FP-LD after it is injection locked by the DFB-FL. Injection locking was achieved by fine-tuning the operating temperature of the FP-LD. When the FP-LD was injection locked, the mode located at 1551.5 nm was amplified by 25 dB. All other sidemodes are strongly suppressed by 20 dB. The sidemodes are also red-shifted by 0.07 nm.⁵ The SMSR of the injection-locked DFB-FL output was 45 dB which can be easily improved to about 65 dB by filtering the laser output with a thin-film bandpass filter. We observed that the linewidth of the injection-locked laser was reduced from 0.3 nm to less than 500 kHz. Heterodyning the injection locked laser



ThGG28 Fig. 1. Experiment setup.